EFFICIENT 3D POISSON SOLVERS FOR SPACE-CHARGE SIMULATION*

J. Qiang†, LBNL, Berkeley, CA 94720, USA

Abstract

Three-dimensional Poisson solver plays an important role in the self-consistent space-charge simulation. In this paper, we present several efficient 3D Poisson solvers inside an open rectangular conducting pipe for space-charge simulation. We describe numerical algorithm of each solver, show comparative results for these solvers and discuss the pros and cons associated with each solver.

INTRODUCTION

Nonlinear space-charge effect in charged particle beam has significant impact to particle beam dynamics in high intensity accelerators. A natural way to include the space-charge effect in the simulation is through self-consistent particle-in-cell (PIC) method [1–4]. In the PIC method, macroparticles are advanced step by step in phase space subject to both the external forces and the space-charge forces. Normally, at each step, the external forces can be quickly computed using the given external fields. The space-charge forces are calculated self-consistently using the charge density distribution at that step by solving the Poisson equation. This involves a large number of numerical operations and is much more computational expensive compared with the external force calculation. An efficient Poisson solver will be of importance in the PIC simulation in order to quickly calculate the space-charge forces and to reduce the total simulation time.

In previous studies, a number of Poisson solvers have been studied subject to different boundary conditions [5–12]. In this paper, we proposed three new Poisson solvers in an open rectangular conducting pipe. Figure 1 shows a schematic plot of charged particle beam inside an open rectangular conducting pipe. Even with the longitudinal open boundary condition, these three Poisson solvers will use a computational domain that longitudinally contains the beam itself. No extra computational domain is needed in the longitudinal direction in order to meet the open boundary conditions on both sides of the beam.

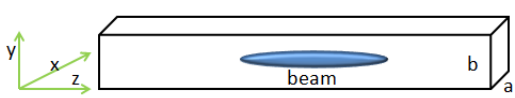

Figure 1: A schematic plot of a charged particle beam inside an open rectangular conducting pipe.

* Work supported by the U.S. Department of Energy under Contract No. DE-AC02-05CH11231.

† jqiang@lbl.gov

NUMERICAL METHODS

For a perfect conducting pipe with rectangular cross section, we write the three-dimensional (3D) Poisson equation as:

$$\frac{\partial^2\phi}{\partial x^2}+\frac{\partial^2\phi}{\partial y^2}+\frac{\partial^2\phi}{\partial z^2}=-\frac{\rho}{\epsilon_0} \tag{1}$$

Here, ϕ denotes the electrostatic potential, ρ the dimensionless charge density function, x, y and z denote the horizontal, vertical, and longitudinal coordinates respectively. The boundary conditions for the potential in the open perfect rectangular conducting pipe are:

$$\phi(x=0,y,z) = 0 \tag{2}$$
$$\phi(x=a,y,z) = 0 \tag{3}$$
$$\phi(x,y=0,z) = 0 \tag{4}$$
$$\phi(x,y=b,z) = 0 \tag{5}$$
$$\phi(x,y,z=\pm\infty) = 0 \tag{6}$$

where a is the horizontal width of the pipe and b is the vertical width of the pipe. In the following, we propose three efficient numerical methods to solve the Poisson equation subject to above boundary conditions.

Spectral-Integrated Green Function Method

Given the boundary conditions in Eq. 2-6, the potential ϕ and the source term ρ can be approximated using two sine functions as:

$$\rho(x,y,z)=\sum_{l=1}^{N_l}\sum_{m=1}^{N_m}\rho^{lm}(z)\sin(\alpha_l x)\sin(\beta_m y) \tag{7}$$

$$\phi(x,y,z)=\sum_{l=1}^{N_l}\sum_{m=1}^{N_m}\phi^{lm}(z)\sin(\alpha_l x)\sin(\beta_m y) \tag{8}$$

where

$$\rho^{lm}(x,y,z)=\frac{4}{ab}\int_0^a\int_0^b\rho(x,y,z)\sin(\alpha_l x)\sin(\beta_m y)\,dxdy \tag{9}$$

$$\phi^{lm}(x,y,z)=\frac{4}{ab}\int_0^a\int_0^b\phi(x,y,z)\sin(\alpha_l x)\sin(\beta_m y)\,dxdy \tag{10}$$

where $\alpha_l = l\pi/a$ and $\beta_m = m\pi/b$. Substituting above expansions into the Poisson equation and making use of the orthnormal conditions of the sine functions, we obtain

$$\frac{\partial^2\phi^{lm}(z)}{\partial z^2}-\gamma_{lm}^2\phi^{lm}(z) = -\frac{\rho^{lm}}{\epsilon_0} \tag{11}$$

ISBN 978-3-95450-173-1

where $\gamma_{lm}^2 = \alpha_l^2 + \beta_m^2$. The above ordinary differential equation for each mode lm can be solved using a Green function method. This solution can be written as:

$$\phi^{lm}(z) = \frac{1}{2\gamma_{lm}\epsilon_0}\int G_{lm}(z-z')\rho^{lm}(z')\,dz' \tag{12}$$

where the Green function G is given by:

$$G_{lm}(z-z') = \exp\left(-\gamma_{lm}|z-z'|\right) \tag{13}$$

The above convolution integral can be discretized on a mesh that longitudinally contains only the beam. The discrete potential on a grid point $z_i, i = 1, \cdots, N_z$ is given as:

$$\phi^{lm}(z_i) = \frac{h_z}{2\gamma_{lm}\epsilon_0}\sum_{j=1}^{N_z} G_{lm}(z_i - z_j)\rho^{lm}(z_j) \tag{14}$$

where $h_z = (z_{max} - z_{min})/(N_z - 1)$, z_{min} is the minimum and maximum locations of the beam along the z direction, and N_z is the number of grid points. The direct brute-force calculation of above summation for all N_z grid data points takes $O(N_z^2)$ operations. Fortunately, by using the zero padding method [12–15], the computational cost of the summation for all N_z data points can be reduced to $O(N_z log(N_z))$.

The Green function given in Eq. 13 is exponentially damped with the increase of the separation between two grid points. In the numerical calculation of Eq. 12, resolving such fast damping may not be necessary if the variation of beam density along z is slow. The convolution integral Eq. 12 can be rewritten as

$$\phi^{lm}(z) = \frac{1}{2\gamma_{lm}\epsilon_0}\sum_j \int_{z_j - h_z/2}^{z_j + h_z/2} G_{lm}(z-z')\rho^{lm}(z')\,dz' \tag{15}$$

If we assume that the charge density ρ^{lm} stays constant within the interval $[z_j - h_z/2, z_j + h_z/2]$, the above equation can be reduced into:

$$\phi^{lm}(z) = \frac{1}{2\gamma_{lm}\epsilon_0}\sum_j G_{lm}^{int}(z - z_j)\rho^{lm}(z_j) \tag{16}$$

where

$$G_{lm}^{int}(z - z_j) = \int_{z_j - h_z/2}^{z_j + h_z/2} G_{lm}(z - t)\,dt \tag{17}$$

Substituting Eq. 13 into above equation, we obtain the integrated Green's function as:

$$G_{lm}^{int}(z_i - z_j) = \begin{cases} \frac{\exp(\gamma_{lm}|z_i - z_j|)}{\gamma_{lm}}(\exp(\gamma_{lm}h_z/2) - \\ \exp(-\gamma_{lm}h_z/2)), \text{ if } i \neq j \\ \frac{2}{\gamma_{lm}}(1 - \exp(-\gamma_{lm}h_z/2)) \text{ otherwise} \end{cases} \tag{18}$$

Using the integrated Green's function G^{int}, the convolution summation Eq. 16 can be calculated using the same zero padding method as the standard Green function method. The advantage of this method is that the fast decrease of the Green function does not need to be resolved in the numerical approximation to the convolution integral 12, which can significantly save computational resources.

The numerical calculation of the sine function transform in both x and y directions can be done efficiently using an FFT method. The computational cost in transverse x and y dimensions scales as $O(N_x N_y N_z(\log(N_x N_y))$. Using the zero padding and the FFT for the cyclic summation, the cost to compute the convolution also scales as $O(N_x N_y N_z log(N_z))$. This results in a total computational cost to solve the 3D Poisson equation in an open conducting pipe scaling as $O(N_x N_y N_z \log(N_x N_y N_z))$.

3D Spectral Method

In many accelerator physics application, the longitudinal density distribution of the charged particle beam has a Gaussian distribution. This suggests that the ordinary differential equation 11 can also be solved efficiently using a Hermite-Gaussian expansion, which naturally satisfies the open boundary conditions (Eq. 6) in the z direction.

The charge density ρ and electrostatic potential ϕ can be approximated as:

$$\rho^{lm}(z) = \sum_{n=0}^{n=N_n} \rho_n^{lm}\mathcal{H}_n(z) \tag{19}$$

$$\phi^{lm}(z) = \sum_{n=0}^{n=N_n} \phi_n^{lm}\mathcal{H}_n(z) \tag{20}$$

where the scaled Hermite-Gaussian function $\mathcal{H}_n$ is defined as:

$$\mathcal{H}_n(z) = H_n(\frac{z}{A})\exp(-\frac{1}{2}\frac{z^2}{A^2}) \tag{21}$$

where A is a longitudinal scaling constant, which can be $A = \sigma_z$ with σ_z the beam longitudinal RMS size, H_n is the n^{th} order Hermite polynomial with properties: $H_0(z) = 1$, $H_1(z) = 2z, \cdots, H_n(z) = 2zH_{n-1} - 2(n-1)H_{n-2}$. The scaled Hermite-Gaussian function $\mathcal{H}$ has the properties:

$$\int_{-\infty}^{\infty}\mathcal{H}_n(z)\mathcal{H}_m(z)dz = 2^n n!\sqrt{\pi}A\delta_{nm} \tag{22}$$

and

$$\frac{\partial^2\mathcal{H}_n}{\partial z^2} = \frac{1}{4A^2}\mathcal{H}_{n+2} + \frac{n(n-1)}{A^2}\mathcal{H}_{n-2} - \frac{2n+1}{2A^2}\mathcal{H}_n \tag{23}$$

where $\delta_{mn} = 1$ for $m = n$ and $\delta_{mn} = 0$ for $m \neq n$. The expansion coefficients ρ_n and ϕ_n can be obtained from

$$\rho_n^{lm} = \frac{1}{2^n n!\sqrt{\pi}A}\int_{-\infty}^{\infty}\rho^{lm}(z)\mathcal{H}_n(z)dz \tag{24}$$

$$\phi_n^{lm} = \frac{1}{2^n n!\sqrt{\pi}A}\int_{-\infty}^{\infty}\phi^{lm}(z)\mathcal{H}_n(z)dz \tag{25}$$

Substituting the functions ρ and ϕ into the Eq. 11, and using the orthogonality of the scaled Hermite-Gaussian functions

ISBN 978-3-95450-173-1

and Eq. 22, the Poisson equation is reduced into a group of linear algebraic equations:

$$\frac{1}{4}\phi^{lm}_{n-2} - (\frac{1}{2}(2n+1) + \gamma^2_{lm}A^2)\phi^{lm}_n + (n+2)(n+1)\phi^{lm}_{n+2} = -A^2\rho^{lm}_n/\epsilon_0 \quad (26)$$

where $n = 1,2,\cdots,N_n$ and N_n is the number of Hermite-Gaussian modes. This group of algebraic equations is a band-limited matrix equation, which can be solved effectively using direct Gaussian elimination with a computational cost of $O(N_n)$ for each transverse mode l and m, which results in a total cost as $O(N_l N_m N_n)$. The computational cost of the sine transform scales as $O(N_x N_y N_z \log(N_x N_y)$. The calculation of the Hermite-Gaussian expansion coefficients are more expensive and scales as $O(N_l N_m N_n N_z)$. If the number of Hermite-Gaussian modes can be controlled within a reasonable limit taking advantage of the high order accuracy of the spectral method, this method can still be very efficient. Another advantage of this method is that it provides a natural smoothing of electrostatic function in the self-consistent particle-in-cell simulation by neglecting the high frequency modes in the expansion.

3D Integrated Green Function Method

Another method to solve the 3D Poisson equation inside the open rectangular pipe is to use an integrated Green function method directly. This method has the advantage of using a computational domain that contains only the beam itself instead of the whole transverse pipe cross-section. The solution of the 3D Poisson equation can be written as:

$$\phi(x,y,z) = \frac{2}{ab\epsilon_0}\sum_{l=1}^{\infty}\sum_{m=1}^{\infty}\frac{1}{\gamma_{lm}}\sin(\alpha_l x)\sin(\beta_m y)\times \int_{x_{min}}^{x_{max}}\int_{y_{min}}^{y_{max}}\int_{z_{min}}^{z_{max}}\sin(\alpha_l x')\sin(\beta_m y')\times \exp(-\gamma_{lm}|z-z'|)\rho(x',y',z')\,dx'dy'dz' \quad (27)$$

The above equation can be rewritten as:

$$\phi(x,y,z) = \frac{1}{2ab\epsilon_0}\int_{x_{min}}^{x_{max}}\int_{y_{min}}^{y_{max}}\int_{z_{min}}^{z_{max}}\sum_{l=1}^{\infty}\sum_{m=1}^{\infty}\frac{1}{\gamma_{lm}}[\cos(\alpha_l(x-x')) - \cos(\alpha_l(x+x'))]\times (\cos(\beta_m(y-y')) - \cos(\beta_m(y+y')))\times \exp(-\gamma_{lm}|z-z'|)\rho(x',y',z')\,dx'dy'dz' \quad (28)$$

Following the same idea of preceding section, we can define a three-dimensional integrated Green's function as:

$$G^{int}_{3D}(x,x',y,y',z,z') = \frac{1}{2ab\epsilon_0}(R(x-x',y-y',z-z') - R(x-x',y+y',z-z') - R(x+x',y-y',z-z') + R(x+x',y+y',z-z')) \quad (29)$$

where

$$R(u,v,w) = \sum_{l=1}^{\infty}\sum_{m=1}^{\infty}\frac{1}{\alpha_l\beta_m}[\sin(\alpha_l(u-h_x/2)) - \sin(\alpha_l(u+h_x/2))]\times (\sin(\beta_m(v-h_y/2)) - \sin(\beta_m(v+h_y/2)))G^{int}_{lm}(w) \quad (30)$$

The discrete potential on a grid (i,j,k) can be written as:

$$\phi(x_i,y_j,z_k) = \sum_{i=1}^{N_x}\sum_{j=1}^{N_y}\sum_{k=1}^{N_z}G^{int}_{3D}(x_i,y_j,z_k,x'_i,y'_j,z'_k)\times \rho(x'_i,y'_j,z'_k) \quad (31)$$

The above summation can also be calculated on a doubled computational domain using an FFT-based zero padding method. In order to compute this summation using the FFT-based method, besides the direct convolution term $R(x-x',y-y',z-z')\rho(x',y',z')$, there are also terms that contain auto-correlation in $R(x-x',y+y',z-z')$, $R(x+x',y-y',z-z')$, and $R(x+x',y+y',z-z')$. It turns out that those auto-correlations can be handled in a similar way to the convolution term except that a backward/forward FFT is used in the dimension with auto-correlation while a forward/backward FFT is used in the dimension of convolution [12]. The computational cost for such cyclic summation scale as $O(N_x N_y N_z \log(N_x N_y N_z))$.

NUMERICAL TESTS

In the following, we show a numerical test example for above proposed algorithms. Here, we assume that the beam has a 3D normalized Gaussian density distribution as:

$$\rho(x,y,z) = \exp(-\frac{(x-x_0)^2}{2\sigma_x^2} - \frac{(y-y_0)^2}{2\sigma_y^2} - \frac{(z-z_0)^2}{2\sigma_z^2}) \quad (32)$$

where σ_x, σ_y, and σ_z denote RMS (root mean square) sizes of the beam, and x_0, y_0, and z_0 denote the centroid of the beam. We assume that the transverse aperture sizes of the pipe $a = b = 2$, transverse RMS beam sizes $\sigma_x = \sigma_y = 1/6$, and $\sigma_z = 100/6$. This results in an aspect ratio $A = 100$ for the beam. The computational grid used in this example is $65 \times 65 \times 64$.

Figure 2 shows the electrostatic potential solution and the relative errors along the central horizontal axis from the above three numerical methods (the spectral-integrated Green's function, the 3D spectral method, the 3D integrated Green's function method) and the analytical solution. All three methods have relative errors below 0.1%. The 3D spectral method has the least relative errors as expected. The 3D integrated Green's function method has the largest relative errors but is still below 0.1%.

Figure 3 shows the electrostatic potential solutions and relative errors along center longitudinal axis in this test example using the three numerical methods together with the analytical solution. All three methods give a good approximation to the analytical solution with the maximum relative error below 0.1%. Again, the 3D spectral method shows the least relative error among the three methods.

ISBN 978-3-95450-173-1

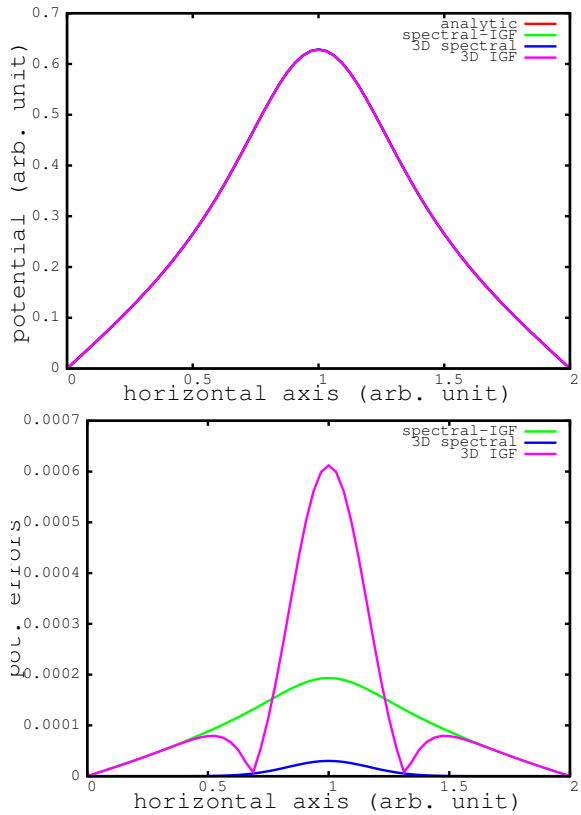

Figure 2: The electrostatic potential solutions (top) and relative errors (bottom) along the horizontal axis from the three proposed numerical algorithms and from the analytical solution.

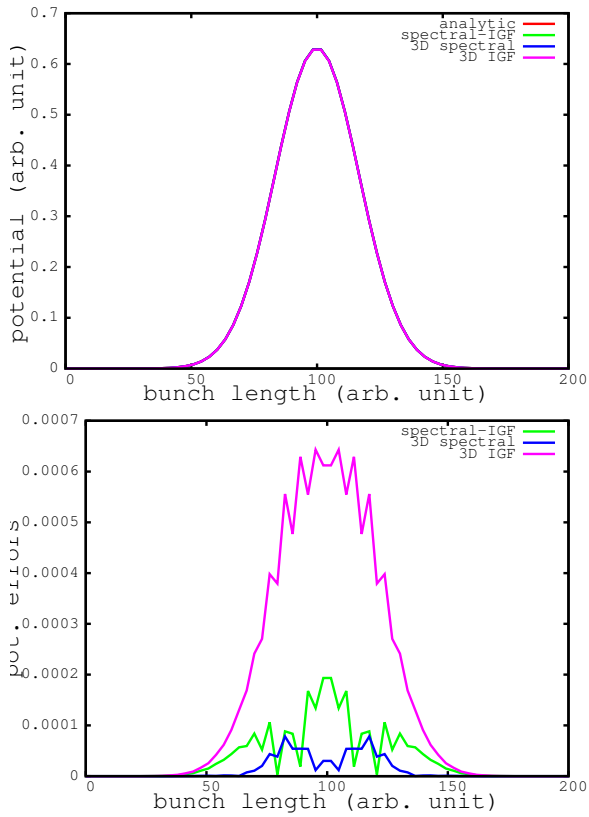

Figure 3: The electrostatic potential solutions (top) and relative errors (bottom) along the longitudinal axis from the three proposed numerical algorithms and from the analytical solution.

CONCLUSIONS

In this paper, we presented three 3D Poisson solvers to calculate the electrostatic potential of a charged particle beam in an open conducting rectangular pipe. Those three Poisson solvers effectively save the computational resource by using a computational domain that longitudinally contains the beam itself. The spectral-integrated Green function solver and the 3D integrated Green function solver have a computational complexity of $O(N\log(N))$, where N is the total number of grid points. The computational cost of the 3D spectral solver scales as $O(N_n N)$, where N_n is the number of Hermite-Gaussian modes used in the solution. Given the fast convergence rate of the spectral solver, the mode number might be kept as small. In the scaling estimation, all these three Poisson solvers are efficient in the numerical operations. In practical application, the 3D integrated Green function method is most time consuming due to the double summation in the calculation of the Green function. However, it has the advantage that the computational domain only needs to contain the beam itself in both transverse and longitudinal directions. This saves computational cost when the transverse size of the beam is much smaller than the transverse pipe aperture. The 3D spectral solver has an extra cost factor depending on the Hermite-Gaussian mode number. However, this solver normally leads to less numerical error and can also provide smooth potential solution when the charge density function contains numerical noise from the discrete macroparticle deposition in the PIC simulation. The spectral-integrated Green function solver has a numerical accuracy between the 3D spectral solver and the 3D integrated Green function solver, but a very favorable computational cost scaling.

ACKNOWLEDGMENTS

This research used resources of the National Energy Research Scientific Computing Center, which is supported by the Office of Science of the U.S. Department of Energy.

REFERENCES

[1] A. Friedman, D.P. Grote and I. Haber, Phys. Fluids **B 4**, 2203 (1992).

[2] T. Takeda, J.H. Billen, "Recent developments of the accelerator design code PARMILA," Proceedings of the XIX International Linac Conference, Chicago, IL, August 1998, pp. 156-158.

[3] J. Qiang, R.D. Ryne, S. Habib, V. Decyk, J. Comput. Phys. **163**, 434 (2000).

[4] J. Qiang, S. Lidia, R.D. Ryne, and C. Limborg-Deprey, Phys. Rev. ST Accel. Beams **9**, 044204 (2006).

ISBN 978-3-95450-173-1

[5] D.B. Haidvogel and T. Zang, J. Comput. Phys. **30**, 167 (1979).

[6] S. Ohring, J. Comput. Phys. **50**, 307 (1983).

[7] H. Dang-Vu and C. Delcarte, J. Comput. Phys. **104**, 211 (1993).

[8] E. Braverman, M. Israeli, A. Averbuch, and L. Vozovoi, J. Comput. Phys. **144**, (1998).

[9] L. Plagne and J. Berthou, J. Comput. Phys. **157**, 419 (2000).

[10] J. Qiang and R.D. Ryne, Comp. Phys. Comm. **138**, 18 (2001).

[11] J. Qiang and R. Gluckstern, Comp. Phys. Comm. **160**, 120, (2004).

[12] R.D. Ryne, "On FFT based convolutions and correlations, with application to solving Poisson's equation in an open rectangular pipe," arXiv:111.4971v1, 2011.

[13] J.W. Eastwood, D.R.K. Brownrigg, J. Comput. Phys. 32 (1979) 24.

[14] W.H. Press, B.P. Flannery, S.A. Teukolsky, W.T. Vetterling, Numerical Recipes in FORTRAN: The Art of Scientific Computing, 2nd ed., Cambridge University Press, Cambridge, England, 1992.

[15] J. Qiang, Comp. Phys. Comm. **181**, 313, (2010).

ISBN 978-3-95450-173-1